ORIGINAL RESEARCH ARTICLE

Fabrication of Refractory Intermetallic Cr_2Ta by Reducing Metal Oxides with Calcium Hydride

S. YUDIN, S. VOLODKO, A. GURYANOV, A. KASIMTSEV, T. SVIRIDOVA, I. ALIMOV, S. KUZOVCHIKOV, A. KONDRATIEV, A. KOROTITSKIY, and D. MOSKOVSKIKH

High-temperature Cr-Cr_2Ta composites are promising candidates for replacing nickel-based precipitation-hardening superalloys for producing turbine blades. Segregation at the solidification of such alloys leads to a dendritic structure, which has a negative impact on the mechanical properties. In order to avoid such issues, powder metallurgy is considered a suitable method. In this work, the theoretical and practical aspects of producing Cr_2Ta by powder metallurgy using metallothermic (calcium-hydride) synthesis of a refractory intermetallic compound from oxide raw materials have been studied. Using X-ray and electron microscopic analysis, it has been established that the formation of the Cr_2Ta phase occurs due to solid-state diffusion of chromium particles in Ta. The apparent activation energy of this process is 291 ± 69 kJ/mol. It has been shown that the diffusion reaction actively occurs at a temperature of only 0.56 T_m of Cr_2Ta. Thermodynamic calculations and thermal analysis have established that such a low temperature of formation of Cr_2Ta is due to heat releasing during the exothermic reduction reaction of Cr_2O_3 oxide by calcium. The optimal synthesis parameters have been determined, and their influence on the phase composition of the powder has been studied. The developed technology makes it possible to obtain Cr_2Ta intermetallic powder containing 95 ± 5 vol pct of the target phase, with a sponge particle morphology and a size of < 20 μm. Typical impurity content has been determined as follows: < 0.28 wt pct for oxygen, < 0.07 wt pct for nitrogen, and < 0.02 wt pct for hydrogen. Thus, the resulting powder can be used for the production of Cr-Cr_2Ta composites.

https://doi.org/10.1007/s11663-024-03018-0

I. INTRODUCTION

HIGH-TEMPERATURE structural alloys are used in various applications at elevated temperatures. These materials are expected to have a high melting point, strength, and hardness at temperatures of at least (0.5–0.6)·T_m,[1] and, additionally, they should possess a combination of a high elastic modulus, high creep resistance, and be resistant to high-temperature oxidation. Alloys based on refractory intermetallic compounds meet these requirements well.[2–6]

To date, more than 200 refractory intermetallic compounds with a melting point above 1500 °C have been discovered and described.[7] Among this variety of intermetallic compounds, the Laves phases, forming by two refractory metals (AB_2, where A = Nb, Ta, Zr, Hf; B = Fe, Co, Cr), hold a special place.[8,9] Such compounds are characterized by a high melting point (> 1500 °C),[10] high hardness at room temperature (HV = 9–13 GPa, load 0.3 kg[11]), high strength, and creep resistance at temperatures > 0.5 T_m.[8,12,13] Such properties allow one to consider this group of materials as the basis for the elaboration of a new generation of high-temperature materials.

In this context, the Cr_2Ta compound, which has a high melting point (2020 °CC[14]) and hardness ($E \approx 200$ GPa, with Poisson's ratio $\mu = 0.360$[15]), seems to be quite promising. Due to the high Cr content, this intermetallic compound has high yield strength at temperatures above ≥ 1100 °C.[16–18] Some physical, mechanical, and thermodynamic properties of

S. YUDIN, S. VOLODKO are with the LLC Metsintez, Tula, Russia, 300041. A. GURYANOV, A. KASIMTSEV, and I. ALIMOV are with the LLC Metsintez and Tula State University, Tula, Russia, 300012. T. SVIRIDOVA is with the LLC Metsintez and National University of Science and Technology MISIS, Moscow, Russia, 119049. S. KUZOVCHIKOV and A. KONDRATIEV are with the Lomonosov Moscow State University, Moscow, Russia, 119991. A. KOROTITSKIY and D. MOSKOVSKIKH are with with the National University of Science and Technology MISIS. Contact e-mail: Sergey-USN@mail.ru; mos@misis.ru

Manuscript submitted April 28, 2023; accepted January 8, 2024.
Article published online March 5, 2024.

Cr_2Ta may be found in the scientific and technical literature.[1,14,15,17,19,20] The properties are summarized in Table S1 (see the electronic supplementary data file).

To reach the potential properties of Cr_2Ta and utilize this compound for producing composites, first, it has to be obtained in a single-phase state with the lowest impurity content. In this regard, the problem of Cr_2Ta synthesis comes to the fore. However, in the literature, there are no works devoted to the production of single-phase Cr_2Ta. Research mainly concerns two-phase alloys $Cr + Cr_2Ta$, compositions close to eutectic. For example, according to,[19,21,22] Cr-7...13Ta (at pct) alloys were produced by vacuum arc or induction melting. However, due to segregation that occurs during the crystallization of Cr–Ta alloys, the ingots solidify into a dendritic structure and, accordingly, have an inhomogeneous chemical composition. In addition, Cr and Ta have different melting and boiling points and vapor pressure,[23,24] which causes the instability of melting under vacuum conditions.

For such complicated in terms of production alloys, the powder metallurgy looks as a promising technology. There are vastly limited studies devoted to the production of $Cr + Cr_2Ta$ alloys by powder metallurgy. Portnoi *et al.*[25] synthesized the Cr-7...11Ta (at pct) alloys additionally doped with W, Zr, Nb, or Si by mechanochemical synthesis. Due to the peculiarities of the synthesis method, powders can become contaminated with the material of the milling media and oxidize. Accordingly, this will negatively affect the reproducibility of the results and the quality of a final product.

In this study, the process of metallothermic (calcium-hydride) synthesis of the refractory intermetallic Cr_2Ta has been studied. In this technology, relatively cheap oxides Cr_2O_3 and Ta_2O stand as raw materials, and CaH_2 is the reducing agent. However, Meyerson[26] showed that the main reducing agent is pure calcium, whereas hydrogen gas formed during the dissociation of the hydride does not lead to the reduction of transitional metal oxides. The CaH_2 is considered to be convenient for the preparation of a homogeneous $Cr_2O_3 + Ta_2O_5 + CaH_2$ mixture due to its brittleness.

For a metallothermic synthesis, an important indicator is believed to be the final oxygen content in a product. For instance, after the magnesiothermic reduction of TiO_2 and ZrO_2, Ti, and Zr contain 2.30 and 1.55 wt pct O.[27,28] According to Kubaschewski[27,28] and Liu,[29] calcium is capable of reducing the thermodynamically strong oxides TiO_2, ZrO_2, or refining of Nb (0.13 wt pct O) to an oxygen content of 0.07, 0.04, and 0.01 wt pct, respectively. Moreover, Cr obtained through the calciothermic reduction has 0.0032 wt pct of O.[30] Thus, the calcium-hydride synthesis is considered a suitable technology for obtaining Cr_2Ta intermetallic and its composites.

Nb_3Al intermetallic,[31] Ti–18Zr-15Nb (at pct) alloy,[32] Hf nanocarbide, and carbonitride[33] have been successfully obtained via the calcium-hydride synthesis at temperatures not exceeding 1200 °C. More details about this technology can be found in.[34] In the scientific literature, no works devoted to the study of the calcium-hydride synthesis process of Cr_2Ta have been found. The specifics of the interaction of reduced metals with each other in a reaction volume containing different amounts of liquid calcium have not been studied yet. In addition, the mechanism of the calcium-hydride synthesis of various intermetallic compounds and alloys remains not studied.

Proper theoretical and practical understanding of the reduction mechanism of Cr_2O_3 and Ta_2O_5 oxides via calcium-hydride will ensure the development of a technology for producing homogeneous Cr_2Ta intermetallic and Cr_2Ta-Cr high-temperature composites at industrial scale. Thus, the aim of the current work is to investigate the synthesis mechanism and establish the optimal technological parameters to accomplish a decent quality of the Cr_2Ta powder.

II. MATERIALS AND METHODS

A. *Calcium-Hydride Reduction*

The synthesis of Cr_2Ta intermetallic compound powders was conducted through the calcium-hydride reduction. The reaction mixture consisted of Cr_2O_3 oxide (≥ 99 wt pct, with an average geometric particle size of 2.54 μm), Ta_2O_5 oxide (≥ 99.8 wt pct, 2.80 μm), and CaH_2 hydride (> 93 wt pct). The initial mixture was mixed in a drum mixer for 30 minutes to achieve homogeneity. The charge composition corresponded to the preparation of 50 g of 35.30 Cr + 64.70 Ta alloy, wt pct (the middle of the Cr_2Ta homogeneity region[14]). The mixed charge was poured into a carbon steel capsule, containing 0.24–0.26 wt pct of carbon, with an inner diameter of 0.036 m, compacted (the density of the charge was 1.6–1.8 g/cm^3), and loaded into a container made of heat-resistant chromium-nickel steel with an inner diameter of 0.11 m. The container was hermetically sealed with a lid, and a vacuum was created to a level of residual gas pressure of 1.33 Pa. After that, argon (purity 99.996 vol pct) was supplied to the overpressure.

The synthesis was carried out in a shaft electric furnace according to the regimes presented in Table I. The recovery time $\tau_r = 0$ means that there was no isothermal holding after the reduction temperature (T_r) was reached and the container immediately began to cool. The heating rate was 10–15 °C/min. After holding, the container was cooled together with the oven to a temperature of 900 °C at an average rate of 22 °C/min. The temperature was monitored by a thermocouple placed near the outer wall of the container.

After the reduction reaction, the removal of calcium and calcium oxide from the products ($Cr_2Ta + CaO + Ca$) was conducted through hydrometallurgical treatment. This involved crushing the resulting reaction products and immersing them in water. After quenching, hydrochloric acid was added to the solution and the acid treatment was carried out for 1 hour at a pH of no more than 2–3. The product was then washed with water to reach a pH of 7 (neutral medium), dried in a vacuum

Table I. Condition of the calcium-hydride synthesis of Cr_2Ta

No*	T_r, °C	τ_r, min	Excess CaH_2, Percent	Capsule for reduction (carbon steel: 0.24–0.26 Weight Percent C)
1	1200	360	0**	new capsule used every time
2			10	
3			20	
4			50	
5			100	
6	970	0	20	
7		240		
8	1000	0		
9		240		
10	1020	240		
11	1050	0		
12		120		
13		240		
14		360		
15	1100	240		
16	1150	0		
17		240		
18	1200	0		
19		120		
20		240		
21		360		
22	1200	360		consecutive syntheses in the same capsule***
23				
24				
25				
26				
27				
28				
29				

*The powders obtained in experiments No. 6-21 were annealed in vacuum at 700 °C before X-ray phase analysis;.
**Zero means the stochiometric content of the reducing agent (CaH_2) according to reaction [1];.
***After each run, the capsule was mechanically cleaned for reuse.

oven at 60 °C, and sieved. The details of the hydrometallurgical processing of the Cr_2Ta powders can be found in Figure S2 (see the electronic supplementary data file).

Figure 1 demonstrates the schematic illustration of the calcium-hydride process.

B. *Analytical Techniques*

X-ray phase analysis was conducted on a DRON-3 automated diffractometer (Burevestnik, Russia) using monochromatic Cu-K_α radiation. The spectra were processed using the software package,[35] which utilized the simplified (reduced) Rietveld method.[36] This allowed for the determination of the volume fractions of the phases and their lattice periods. The relative errors in determining the volume fractions of the phases are 5 vol pct, and the lattice periods are $\Delta a/a = 0.0015$. The samples of powders No. 6-21 (Table I) before X-ray phase analysis were subjected to vacuum annealing at a temperature of 700 °C for 20 minutes under vacuum not worse than 5×10^{-5} mm Hg to remove dissolved hydrogen, which dissolves in Ta causing the broadening of Bragg's reflections in X-ray profiles. The integral concentration of interstitial impurities (O, N, C, H) was determined by a CS-600 carbon analyzer (Leco), a TC-600 oxygen and nitrogen analyzer (Leco), and RHEN-602 hydrogen analyzer following standard methods. The structure of the samples was investigated using a JSM7600F scanning electron microscope (JEOL, Japan) equipped with an X-ray microanalysis system (EDX, Oxford Instruments). To simulate the conditions of the calcium-hydride reduction, the powder mixtures of $Cr_2O_3 + CaH_2$ (120.71 mg), $Ta_2O_5 + CaH_2$ (107.54 mg), and $Cr_2O_3 + Ta_2O_5 + CaH_2$ (214.51 mg) were heated in a Labsys differential scanning calorimeter (DSC) EVO (Setaram, France) equipped with a high-sensitivity CALVET type Cp-rod. A 20 pct excess of calcium hydride was added. The study was conducted in the temperature range of 600–1200 °C. The crucibles used were made of carbon steel (0.24–0.26 wt pct C) as in the traditional metallothermic process. In addition, the thermodynamic stability of the synthesized Cr_2Ta powder was also evaluated in Al_2O_3 crucibles on a Labsys EVO device with a TG-DTA sensor, in the temperature range of 800–1250 °C, with a temperature control accuracy of ± 1 °C. The setup was calibrated to the following standards: Sn (99.9995 wt pct), Al (99.995 wt pct), Ag (99.99 wt pct), Cu (99.999 wt pct), and Ni (99.99 wt pct). In both types of DSC

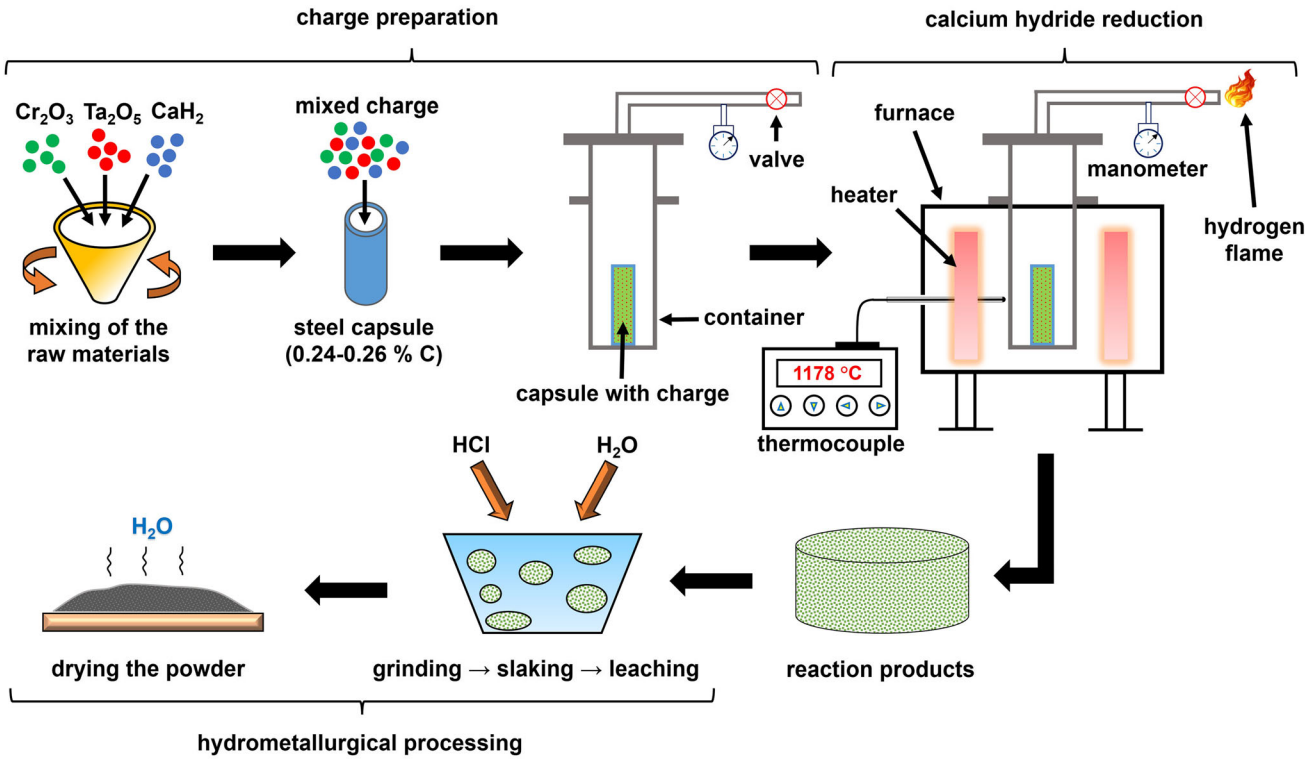

Fig. 1—Schematic illustration of Cr_2Ta synthesis.

experiments, the heating and cooling rates were 10 °C/min and the atmosphere was flowing argon with a purity of 99.998 vol pct.

Statistical analysis of the experimental data was performed using Minitab 21 software. A regression model was constructed for obtaining of Cr_2Ta via the calcium-hydride synthesis, taking into account the statistical significance of each technological factor. The least-squares method was utilized for this purpose, with the independent factors being the temperature and time of synthesis, the amount of excess reducing agent, and the number of runs (Table I, No. 22-29) in the same reaction capsule (Runs). Upon each run, the capsule was mechanically cleaned, then another mixture (Cr_2O_3 + Ta_2O_5 + CaH_2) was loaded, and the next run was started. The model also considered the multiplicative effect of these factors on the yield of the Cr_2Ta phase.

C. *Results and Discussion*

The reaction of obtaining Cr_2Ta by the calcium-hydride reduction of Cr_2O_3 and Ta_2O_5 oxides can be represented as follows:

$$2Cr_2O_3 + Ta_2O_5 + 11CaH_2 \rightarrow 2Cr_2Ta + 11CaO + 11H_2\uparrow. \quad [1]$$

However, reaction [1] is more complex and consists of several transformations. The decomposition of calcium hydride into Ca and H_2 ($T > 600$ °C[37]) leads to the melting of Ca ($T_m = 839 \pm 2$ °C; hydrogen raises the melting point of Ca to ~ 900 °C[38]). This is followed by the reduction of oxides to pure metals (Cr and Ta) and the subsequent interaction of these reduced metals, resulting in the formation of an intermetallic compound ($2Cr + Ta \rightarrow Cr_2Ta$). In practice, calcium hydride is always added in excess, meaning that the interaction of Cr and Ta takes place in the presence of calcium melt.

D. *Influence of Excess Reducing Agent on the Formation of Cr_2Ta*

In order to evaluate the effect of CaH_2 excess on the reduction process and the phase composition of Cr_2Ta powder, a series of experiments was carried out, where the excess was varied from 0 (no excess) to 100 wt pct of the theoretically required for the complete reduction of Cr_2O_3 + Ta_2O_5 oxides (No. 1-5, Table I). It is worth noting that with an increase in the excess of CaH_2, the amount of Ca melt and hydrogen gas, forming during synthesis, increases (the right side of Eq. [1]).

Figures 2a shows the effect of the excess on the oxygen and nitrogen content in the Cr_2Ta powders. In the initial charge, oxygen is in the form of Cr_2O_3 and Ta_2O_5 and varies from ~ 10.5 to 14.5 wt pct depending on the amount of CaH_2. Figures 2a demonstrates that calcium effectively reduces the oxides Cr_2O_3 and Ta_2O_5. Moreover, regardless of the amount of CaH_2, the residual oxygen concentration in Cr_2Ta powders is at the level of 0.25 wt pct, that is, it drops by two orders of magnitude relative to its content in the charge. According to,[39,40] Ta and Cr_2Ti powders containing ~ 0.3 wt pct oxygen have been successfully obtained under the conditions of the calciothermic reduction of Ta_2O_5 or Cr_2O_3 and TiO_2

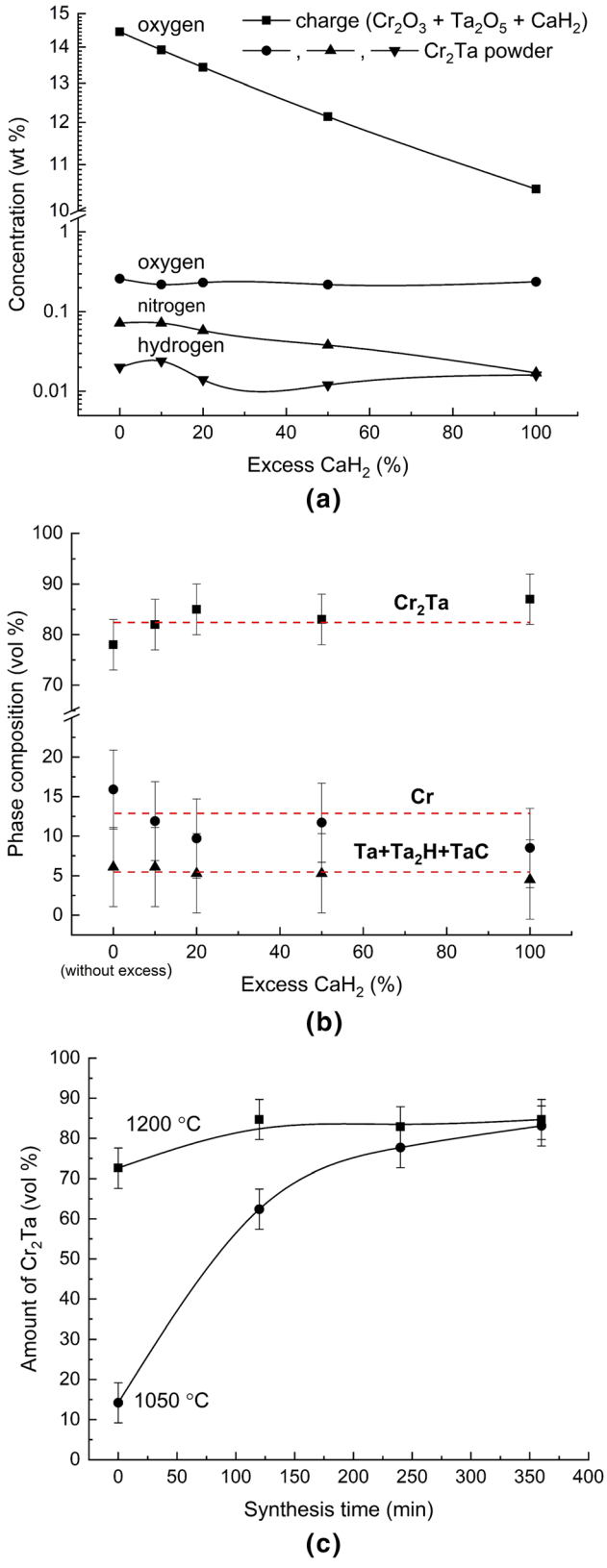

Fig. 2—(*a*) Effect of CaH_2 excess on the oxygen and nitrogen contents in the Cr_2Ta powders; (*b*) Influence of excess reducing agent on the content of the Cr_2Ta phase in synthesis products (the rest is Cr, Ta, and TaC); (*c*) Kinetics of the Cr_2Ta phase formation at two reduction temperatures.

via $CaCl_2$. Thus, our results (Figures 2a) adequately correlate with the literature data. The nitrogen content in the calcium-hydride Cr_2Ta powders is on average 0.05 wt pct.

It can be seen in Figure 2b that regardless of the amount of excess reducing agent (0–100 pct), the amount of Cr_2Ta phase in the synthesized powders is at the level of 80–90 vol pct. It can be concluded that without an excess of the reducing agent (0 pct), the amount of Cr_2Ta phase is slightly less than in the case where there is an excess of CaH_2 (10–100 pct). However, taking into account the accuracy of X-ray phase analysis, it can be assumed that the effect of the liquid calcium phase on the yield of the Cr_2Ta phase is not significant.

Tantalum hydride and carbide have been observed in the synthesized powder (Figures 2b). The formation of TaH_2 is due to the interaction of hydrogen and unreacted tantalum during synthesis, that is, the TaH_2 is retained after synthesis since the powders (runs No. 1-5, Table I) have not been annealed in vacuum. The reasons for the formation of TaC are going to be described below.

Thus, the CaH_2 excess does not have a noticeable effect on the phase composition of the synthesized Cr_2Ta powders and impurity content. In an effort to establish the probable mechanism for the formation of the Cr_2Ta phase under the conditions of the calcium-hydride reduction, a series of experiments was conducted, where the temperature–time parameters of synthesis were varied while maintaining a constant level of the excess reducing agent at 20 pct (experiments 6-21 in Table I). This excess is necessary in order to compensate the dissociation of CaH_2 in air, forming CaO or/and $Ca(OH)_2$ when grinding and mixing.

E. *Effect of temperature and reduction time on the formation of Cr_2Ta*

Figures 2c illustrates the time-dependent growth of the Cr_2Ta phase at the reduction temperatures of 1050 and 1200 °C. As observed in Figures 2c, an increase in isothermal holding time at 1050 °C results in a monotonic increase in the amount of Cr_2Ta phase from approximately 15 to 80 pct by volume.

At a temperature of 1200 °C, about 75 pct vol of the Cr_2Ta phase forms during the heating stage, and only 5–10 pct additionally forms at holding up to 360 minutes, resulting in 80–90 pct vol in total. It can be reasonably concluded that the holding time has a significant effect on the yield of the Cr_2Ta phase only at a synthesis temperature of 1050 °C.

The phase content of the synthesized powders (No. 6-21, Table I) is summarized in Table S3 (see the electronic supplementary data file).

The phase growth kinetic curve presented in Figures 2c allows for the evaluation of the laws and mechanisms that govern the formation of the Cr_2Ta phase at 1050 °C during the calcium-hydride reduction of Cr_2O_3 and Ta_2O_5 oxides. One widely known rule, known as the square root of the reaction time rule, states that if the phase growth is directly proportional to the square root

of the interaction time, then the process is controlled by solid-phase diffusion.[41–43] Other kinetic laws of solid-phase reactions, such as those controlled by the displacement of phase boundaries and diffusion reactions, have also been described in the literature.[44] By rearranging the time dependencies of the amount of phase α (degree of transformation) in special coordinates, it is possible to estimate the mechanism of phase formation[44].Figure 3 shows the results of the rearrangement of the kinetic dependence of the increase in Cr_2Ta at a temperature of 1050 °C, where the volume fraction of the Cr_2Ta phase is represented in relative units as the index of transformation of the substance (α).

As illustrated in Figure 3, the dependence of the formation of Cr_2Ta on the calcium-hydride synthesis appears to follow the square root of time rule, indicating that the process is subject to solid-phase diffusion. Based on the R^2 values, most probably diffusional formation mechanism is controlled by three-dimensional transport process, as it is shown in Figures 3b.

Our analysis of the kinetic laws of Cr_2Ta formation, as reported by,[44] indicates that the experimental data at 1050 °C are best explained by solid-state diffusion processes. Furthermore, the scanning electron microscopy analysis of the surface of the thin sections of Cr_2Ta powders obtained at 1050 °C (as shown in Figure 4) further supports this conclusion. In addition, energy-dispersive analysis (EDS) data reveal that the Cr_2Ta phase obtained at 1050 °C has an average chemical composition of Cr + (35.46 ± 1.09) at pct Ta, with a relatively small compositional variation coefficient of ~ 5.5 pct. This composition of the Cr_2Ta compound is in consistent with the binary state diagram of Cr-Ta, as reported by.[14] The results of X-ray microanalysis are represented in Table S4 (see the electronic supplementary data file).

Determining the chemical composition of individual particles of the Ta(Cr) solid solution is challenging due to the small size of the particles (up to 2 μm), which is comparable to the size of an electron probe. This can cause the excitation of characteristic chromium radiation from nearby individual Cr_2Ta or Cr particles, particularly when assessing the chemical composition of Ta core inside two-phase particles based on Cr_2Ta. In addition, separated and large Cr particles are characterized by a very low content of Ta of 1–2 at pct. This is consistent with the Cr–Ta phase diagram,[14] which indicates that tantalum does not actually dissolve in chromium.

As can be seen in Figures 4(a, b, and d), the synthesized powders contain two-phase particles consisting of the Cr_2Ta matrix and the cores of the Ta(Cr) solution. The size of these particles is typically a few microns or less. The presence of such a structure indicates that the process of Cr_2Ta formation is governed by the diffusion of reduced Cr into Ta particles, especially when considering the greater solubility of Cr in Ta than Ta in Cr, as reported by.[14] However, this structure is quite sudden considering classical diffusional saturation, whereby at a certain stage of interaction, only one Ta core should have been preserved in the center, surrounded by a layer of Cr_2Ta. The probable reason for the formation of two-phase Cr_2Ta particles with several Ta(Cr) cores is the features of solid-phase diffusion in powder bodies, such as

- Diffusion of Cr into a sample (in this case, a reduced Ta powder) of a finite size ($0 < x < l$);
- Contact between reduced metals (Cr and Ta) being at point;
- Complex shape of reduced Ta particles;
- A limited and decreasing source of chromium over time.

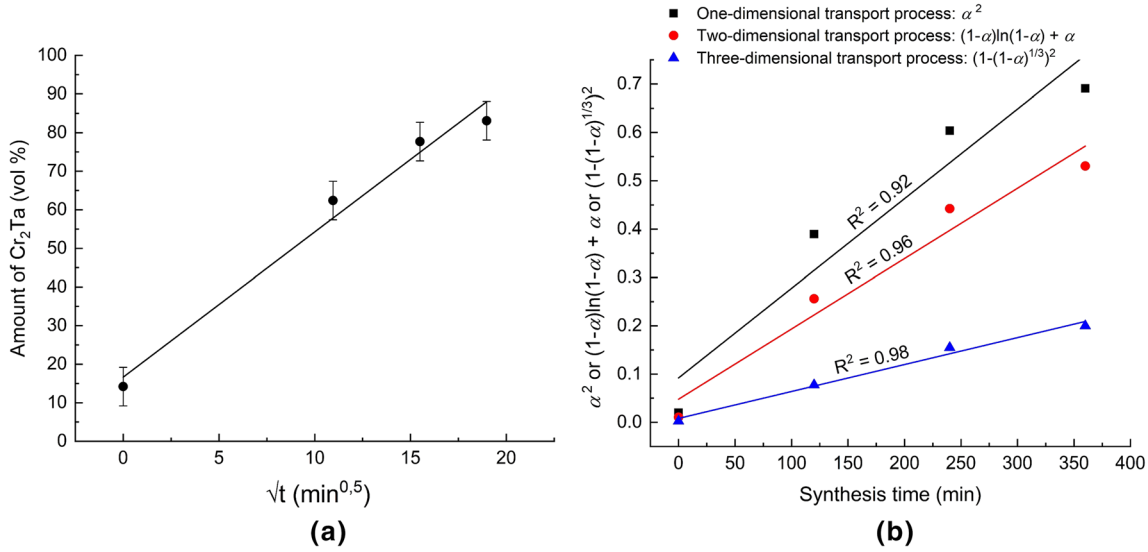

Fig. 3—The rule of the square root of the reaction time (*a*) and the kinetic law of the formation of the Cr_2Ta phase (*b*).

The conditions for such interaction can arise from the limited and concentrated diffusion contact between the powders of the reduced metals in some local volumes (pores) within the refractory oxide CaO, which forms after the calcium-hydride reduction of Cr_2O_3 and Ta_2O_5. Indeed, as reported by,[45] using scanning electron microscopy methods, it has been experimentally shown that in the case of the U-10 wt pct Mo alloy obtained by the calcium-hydride synthesis, the metal particles are located precisely within the pores of CaO and contact each other pointwise (until the moment of uranium melting). Therefore, the final homogeneity of the melt is determined by the local chemical homogeneity of the metals (U and Mo) in a particular CaO pore. The Supplementary File (see electronic supplementary Figure S5) presents illustrative material taken from,[45] demonstrating the structure of the products of the calciothermic reduction of the U-10 wt pct alloy Mo.

In our case, neither Cr nor Ta melts or dissolves in liquid calcium. The entire process takes place in the solid state. Therefore, the completeness of the diffusion interaction between reduced Cr + Ta → Cr_2Ta will be determined by the particle contact area and the local Cr/Ta ratio within the pores in the CaO matrix. Based on this, it is possible to develop a scheme of the formation of two-phase Cr_2Ta particles (Figure 5).

The active reduction of Cr_2O_3 and Ta_2O_5 oxides begins at the moment of the melting of calcium formed after the thermal dissociation of CaH_2 (Figure 5, stage I). This can be demonstrated by heating the mixture of Cr_2O_3 and Ta_2O_5 with CaH_2 in a calorimeter. As a result, CaO and particles of reduced metals Cr and Ta are formed, which are located in the pores of CaO (Figure 5, stage II). If metal particles come into contact with each other, under certain temperature–time conditions, their diffusion interaction will begin (Cr → Ta) and lead to the formation of a Cr_2Ta layer. If all

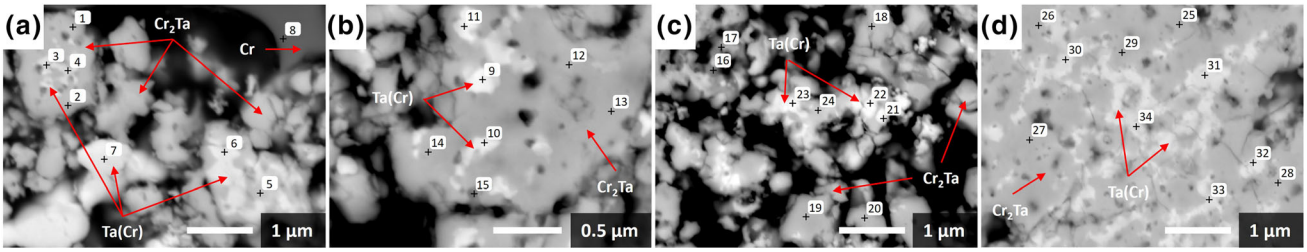

Fig. 4—Electron microscopic study of the structure of Cr_2Ta powders obtained by calcium-hydride reduction of Cr_2O_3 and Ta_2O_5 at 1050 °C for (*a*) 120 min; (*b*) and (*c*) 240 min; (*d*) 360 min.

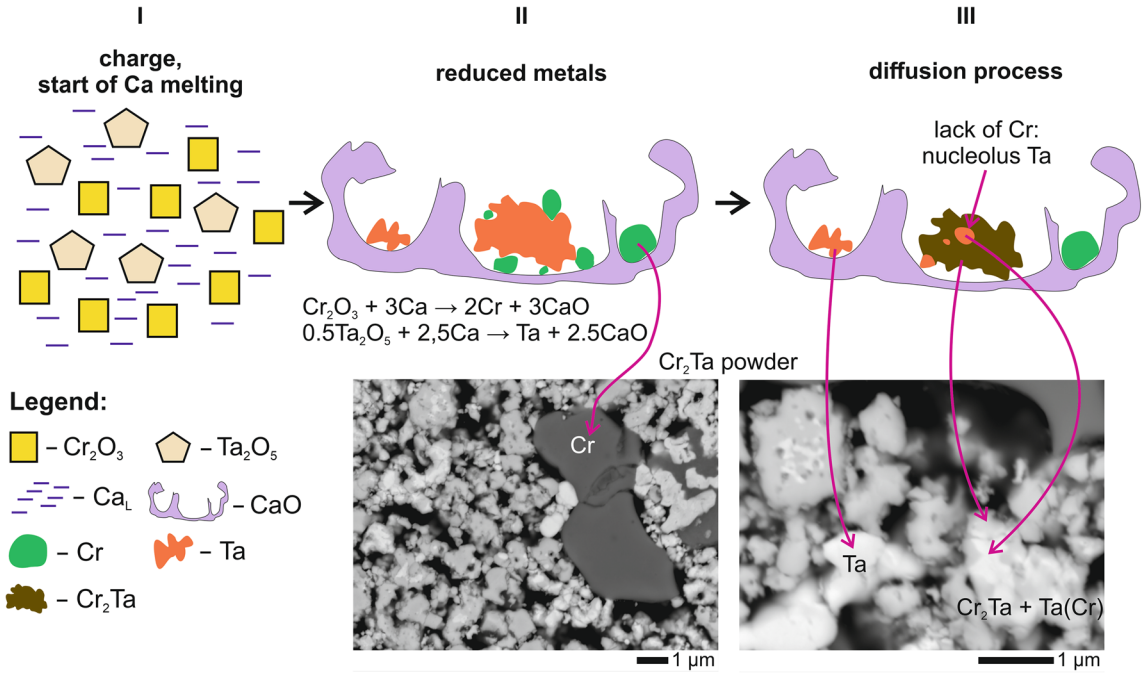

Fig. 5—Scheme of the formation of two-phase particles Cr_2Ta + Ta(Cr) under the conditions of the calcium-hydride reduction of Cr_2O_3 and Ta_2O_5.

conditions are met, then particles consisting only of Cr_2Ta are formed, but even if a condition does not match (for example, the concentration of chromium is not sufficient), then the diffusion reaction does not reach completion, and two-phase particles are formed. Veinlets or cores of Ta(Cr) form due to the limited and unevenly distributed source of diffusible Cr over the surface of Ta particles. At the contact points, the Cr_2Ta phase grows, but not at a distance from them (Figure 5, stage III).

This interpretation of the diffusion formation of two-phase Cr_2Ta/Ta(Cr) particles is supported by the data of electron microscopy analysis. Figures 4b shows large single-phase Cr_2Ta particles (see spectra 10, 11, and 12). The same powder contains equivalent in size, but two-phase Cr_2Ta/Ta(Cr) particles (Figures 4b). Consequently, the phase composition of the particles is determined by the content of Cr and Ta inside CaO pores.

Qi *et al.*[46] have observed a similar two-phase particle structure in calciothermic $Co_{17}Nd_2$ powders, in which a $Co_{17}Nd_2$ intermetallic layer grows on the surface of solid Co particles following diffusion kinetics, as evidenced by the presence of a cobalt core within the cross section of a single particle (see electronic supplementary Figure S6). This ''spotted'' microstructure has also been observed in other systems, such as oxide systems, where during the solid-phase reaction between Al_2O_3 and TiO_2, particles with unreacted TiO_2 cores are observed (see electronic supplementary Figure S7).[47]

It has been established that the formation of the Cr_2Ta phase during the calcium-hydride reduction of Cr_2O_3 and Ta_2O_5 is controlled by solid-phase diffusion. However, at a reduction temperature of 1200 °C, the rate of Cr_2Ta synthesis is so high that most of the desired phase is formed under non-isothermal conditions when heated between 1050 and 1200 °C (as seen in Figure 2c). Meanwhile, holding at 1200 °C provokes a negligible increase in Cr_2Ta amount. To study this phenomenon, the dependence of Cr_2Ta content on the reduction temperature was studied for two holding times (as seen in Figures 6a).

Figures 6a shows that the heat treatment (reduction) of the mixture of $Cr_2O_3 + Ta_2O_5 + CaH_2$ at temperatures > 1000 °C and a holding time of 240 minuters leads to a sudden increase in the amount of the Cr_2Ta phase in the powder (curve 1). However, if there is no exposure at each reduction temperature, then a monotonic increase in the Cr_2Ta phase is observed (curve 2). One can assume that curve 2 in Figures 6a reflects the amount of the intermetallic compound formed during the heating stage (non-isothermal conditions), and curve 1—the amount of Cr_2Ta formed both during the heating process and during holding for 240 minutes at a specific temperature (isothermal conditions). Accordingly, by subtracting curve 2 from curve 1, we can, to a first approximation, estimate the content of the Cr_2Ta phase formed under isothermal reduction conditions (Figures 6b).

Figures 6b reveals that a temperature range of 1050–1100 °C is crucial for the formation of the Cr_2Ta phase. When the reduction temperature rises above 1050 °C, the formation rate of the Cr_2Ta intermetallic becomes so intensive that most of the target phase forms already at the heating stage. If consider that under the conditions of the calcium-hydride synthesis, this compound is formed owing to solid-state diffusion (Figure 3), then such an increase in the rate of formation of Cr_2Ta is probably associated with an additional heating source from the exothermic reduction reaction of Cr_2O_3 and Ta_2O_5 oxides by CaH_2. Such heating of the charge, which can be fully realized during isothermal holding, explains the formation of a large amount of the intermetallic compound (~70 vol pct) at a temperature of 1020 °C, which is only 0.56 of the melting point of Cr_2Ta (Figures 6a, curve 1). In other words, the temperature in the reaction mixture rises without an excess external heat source, which promotes the reduction and further synthesis of a product.

The presence of a critical reduction temperature is confirmed by the observation that after placing the container with the reaction charge into the furnace at a temperature of about 800 °C, the hydrogen flame always ignited. As the furnace temperature, monitored by an external thermocouple, approached 980–1000 °C, the

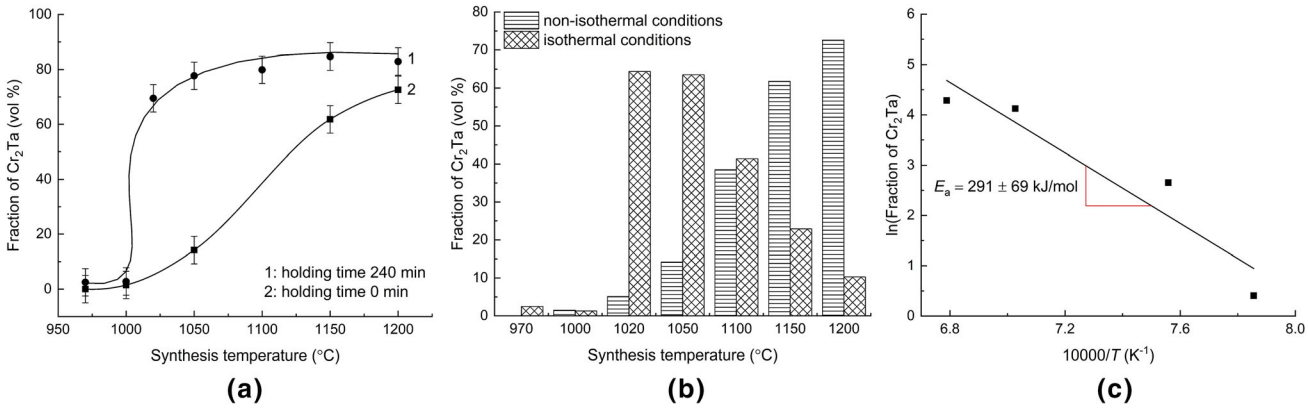

Fig. 6—Effect of reduction temperature on (*a*) amount of Cr_2Ta phase at different holding times; (*b*) the amount of Cr_2Ta phase formed under isothermal and non-isothermal conditions. (*c*) Calculation of the apparent activation energy of calcium-hydride synthesis of the Cr_2Ta phase in the temperature range of 970–1200 °C (experiments without isothermal holding).

hydrogen pressure in the container and, consequently, the burning intensity of the torch increased sharply. However, after reaching 1040–1050 °C, the rate of hydrogen evolution noticeably decreased. This is likely due to the fact that the decomposition of CaH_2 hydride is a thermally activated process; thus, in the temperature range of 980–1040 °C, the temperature of the reaction mixture increased abnormally. It is worth noting that the temperature region of intense evolution (combustion) of hydrogen coincides well with the temperature limit of the jump in the amount of the Cr_2Ta phase (as seen in Figures 6a, curve 1).

An approximation of the apparent activation energy of Cr_2Ta formation was also determined. The Arrhenius plot of the temperature dependence of the Cr_2Ta phase content for experiments without holding (non-isothermal conditions) is shown in Figures 6c. The calcium-hydride synthesis of the Cr_2Ta phase in experiments without holding (as seen in Figures 6c) proceeds according to one mechanism with an activation energy of $E_a = 291 \pm 69$ kJ/mol since the logarithm of the Cr_2Ta content vs $1/T$ is a straight line with $R^2 = 0.90$.

For comparison, Table S8 (see the electronic supplementary data file) shows a comparison of the calculated apparent activation energy in the current work with the activation energies of diffusion processes in various Laves phases.[48–52] This comparison reveals that the present E_a value is close to the activation energies of heterodiffusion in various Laves phases, particularly the chemical analog of Cr_2Nb. This confirms that the formation of Cr_2Ta is controlled by solid-state diffusion in the calcium-hydride synthesis. The Arrhenius plot (as seen in Figures 6c) allows the constructing a mathematical model of the dependence of Cr_2Ta content on the reduction temperature:

$$Q_{Cr_2Ta} = (2.309 \pm 0.491) \cdot 10^{12} \cdot \exp\left(-\frac{(291000 \pm 61000)}{R \cdot T}\right), \quad [2]$$

where Q_{Cr2Ta} is Cr_2Ta content, vol pct; R is the universal gas constant, J/mol·K; T is the reduction temperature, K.

According to model (2), under the given synthesis conditions (the size of reduced Cr and Ta particles is important), the formation of 100 pct of the Cr_2Ta phase is possible at a temperature of ~ 1190 °C. However, as seen in Figures 6a, this is not entirely true. Further, this inconsistency is going to be explained from the point of view of the technological impurity of carbon, which locally changes the chemical composition of the alloy.

The same procedure for the synthesis regimes with an isothermal holding of 240 minutes (as seen in Figures 6a after the jump in the phase composition) does not make physical sense, since the main increase in the Cr_2Ta phase occurs even at the stage of heating and cooling with an activation energy of 291 ± 69 kJ/mol (as seen in Figures 6c). At the longest holding, the additional heating of the reaction mixture starts to have an obvious effect at a reduction temperature over 1000 °C. This indicates that the formation of Cr_2Ta will proceed quickly and with less energy consumption. This activation energy will not reflect the diffusion nature of alloy formation and will depend only on the rate of oxide reduction reactions.

With the aim of testing the hypothesis about the presence of an additional heat source during the synthesis reaction of Cr_2Ta (1), standard thermodynamic calculations and assessment of the thermal effects occurring in mixtures of $Cr_2O_3 + CaH_2$, $Ta_2O_5 + CaH_2$ and $Cr_2O_3 + Ta_2O_5 + CaH_2$ at heating have been carried out using differential scanning calorimeter (DSC). As previously established by Meyerson *et al.*[26], the reducing agent in the calcium-hydride method is calcium, not hydrogen. Recent studies[53–55] have also indicated that the reduction process begins actively after the melting of calcium, which is formed after the thermal dissociation of CaH_2. The decomposition of calcium hydride consumes energy to break the Ca–H chemical bond, resulting in different thermal effects for purely calciothermic and calcium-hydride processes. Table S9 (see the electronic supplementary data file) summarizes the results of the standard thermodynamic calculations of the reduction of Cr_2O_3 and Ta_2O_5, and Cr_2Ta synthesis for these two reducing agents. Thermodynamic data for the calculations were taken from.[20,56]

Of particular interest in the metallothermic process is the specific thermal effect or thermality (q), which represents the calorific value of the reaction mixture. It is generally assumed that the optimal range of thermality for the calcium-hydride synthesis reactions is from ~ 200 to ~ 500 kJ/kg of charge.[57] Within this interval, the process proceeds calmly without explosion. However, if thermality exceeds 500 kJ/kg of charge, the reaction proceeds actively, resulting in the intensive heating of the charge and even the possibility of explosion. To further clarify the data, a histogram (Figure 7) has been included to represent the thermality values from Table S9 (see the electronic supplementary data file). Figure 7 illustrates that pure calcium reduces Cr_2O_3 and Ta_2O_5 oxides with a very high heat release and the reaction of the calciothermic synthesis of Cr_2Ta

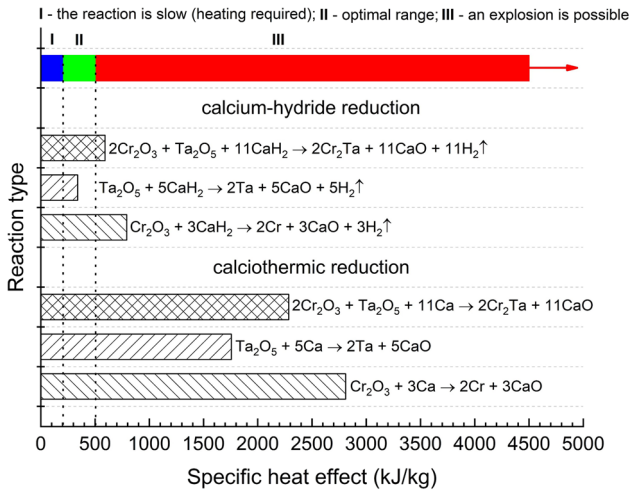

Fig. 7—Specific thermal effect of reduction reactions of Cr_2O_3, Ta_2O_5 and synthesis of Cr_2Ta in calciothermic and calcium-hydride processes.

proceeds with high thermality. The high exothermic effect in such processes poses a safety risk as it can potentially cause an explosion of the charge.

On the other hand, reactions with calcium hydride proceed more smoothly as it is a chemical compound. However, the reduction of Cr_2O_3 oxide and the synthesis of Cr_2Ta still proceed in the heating mode, and the optimal range is exceeded, similar to the calciothermic process. In practice, as previously mentioned, at reduction temperatures of 980–1000 °C, the hydrogen pressure in the container increases sharply resulting in an increase in the combustion intensity of the hydrogen torch, which can only be attributed to the additional heat released during the reduction of Cr_2O_3 with calcium hydride.

The decomposition of CaH_2 and the formation of Cr_2Ta during reduction above 1000 °C are likely driven by the exothermic heat. To test this hypothesis, a series of Differential Scanning Calorimetry (DSC) experiments was conducted using mixtures of $Cr_2O_3 + CaH_2$ (120.71 mg), $Ta_2O_5 + CaH_2$ (107.54 mg), and $Cr_2O_3 + Ta_2O_5 + CaH_2$ (214.51 mg). These samples were heated at a rate of 10 °C/min. It should be noted that the composition of the resulting products was not analyzed at this stage of the study. When CaH_2 is heated, two transformations occur: the polymorphic α-$CaH_2 \rightarrow \beta$-CaH_2 at approximately 800 °C,[58] and the melting of the Ca(H) solid solution, which occurs in the range of 840–900 °C.[38] According to,[30] pure calcium begins to melt at approximately 850 °C. These phase transformations were also observed during the heating of the samples under study (Figures 8a). For the case of the reduction of Ta_2O_5 and a mixture of $Cr_2O_3 + Ta_2O_5$, the moment of calcium melting corresponds to an exothermic peak. However, the main exothermic effect from the reduction of individual oxides or their mixture appears after the appearance of a Ca-based liquid phase, and this is especially clearly seen for the $Cr_2O_3 + CaH_2$ sample. The length of such exothermic peaks can reach up to hundreds of degrees and ends in the temperature range of 950–1000 °C. It was expected that the exothermic effects during heating of the $Cr_2O_3 + Ta_2O_5 + CaH_2$ mixture would be a superposition from the reduction of Cr_2O_3 and Ta_2O_5, but this is not entirely true. This is likely due to the methodological features of the experiment and the high reactivity of ground CaH_2 hydride, which could be oxidized even at the stage of sample preparation or storage. It has been previously shown in[59] that the calciothermic reduction of Ta_2O_5 to pure Ta occurs in a series of successive stages: $Ta_2O_5 \rightarrow CaTa_4O_{11} \rightarrow CaTa_2O_6 \rightarrow Ca_2Ta_2O_7 \rightarrow Ca_4Ta_2O_9 \rightarrow Ta$. The observed sequence of the exothermic peaks during the reduction of Ta_2O_5 with calcium hydride (Figure 11) is likely a result of this stepwise reduction process. The same applies to the calciothermic reduction of Cr_2O_3,[30] which proceeds through the intermediate $CaCr_2O_4$ phase.

In the technology of self-propagating high-temperature synthesis (SHS), there is a solution for obtaining low-exothermic alloys through thermally coupled reactions. If the heat generated during the interaction of the metal components of the desired alloy is not sufficient to initiate the combustion process, a strong exothermic reaction can be added to the system, the products of which should not react with the resulting material. For example, in[60,61] the SHS production of high-entropy metal alloys, $Ti + C \rightarrow TiC + heat\uparrow$ is used as such an exothermic reaction. This releases enough heat that the metal components of the CoCrFeNiMn alloy can melt. In our case, such a source of chemical heat is the reaction $Cr_2O_{3solid} + 3Ca_{liquid} \rightarrow 2Cr_{solid} + 3CaO_{solid} + heat\uparrow$.

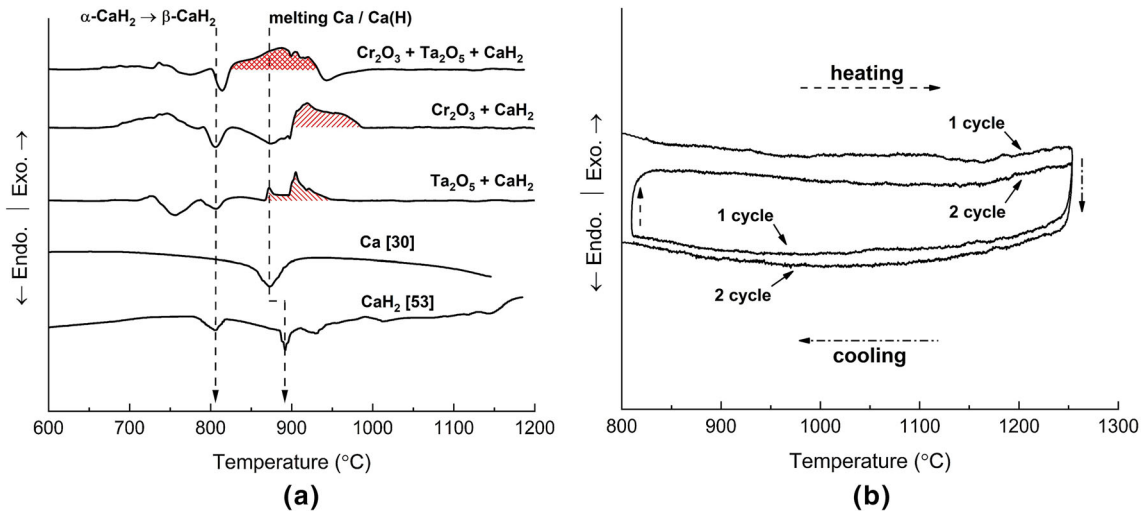

Fig. 8—(*a*) thermal effects in the reduction of Cr_2O_3 and Ta_2O_5 with calcium hydride; (*b*) thermal cycling of Cr_2Ta powder, synthesized at a temperature of 1200 °C with an isothermal holding of 120 min, in the temperature range of 800–1250 °C. Powder phase composition: 83 Cr_2Ta + 9 Cr + 8 (Ta_2C + TaC), vol pct.

To eliminate the possibility of any other mechanism of the interaction between Cr and Ta leading to the formation of Cr_2Ta, such as eutectoid or peritectoid reactions, thermal cycling of the Cr_2Ta powder synthesized at 1200 °C was conducted for 120 minutes. The results are presented in Figures 8b. Figures 8b demonstrates that there are no thermal effects on all heating and cooling cycles. This indicates that there are no invariant transformations in the Cr_2Ta phase, making it thermodynamically stable. Additionally, there is no interaction between impurity phases (Cr, TaC, Ta_2C) or with Cr_2Ta.

F. *Morphology of Calciothermic (Calcium-Hydride) Powders*

The morphology of calciothermic (calcium-hydride) powders of intermetallic compounds, solid solutions, and other compounds provides valuable information about their formation mechanism. For example, metal crystals that grow from a liquid phase or from a gaseous phase are distinguished by their regular geometric shape: a cube or prism with a triangular or polyhedral base.[62] The shape of a crystal is determined by the type of its crystal lattice and the surface energy of various crystallographic faces, primarily of the (111), (101), and (100) planes.[62] Then we can conclude that if particles of regular shape are formed by the calciothermic reduction of oxides, then this alloy is formed due to the dissolution-nucleation of its components through a Ca melt. It is obvious that the action of this mechanism is determined by the solubility of elements in liquid calcium. Table S9 (see the electronic supplementary data file) summarizes the solubility for some metals (insoluble: Ti,[63] Zr, Hf, V,[64] Nb,[64,65] Cr[66]; soluble: Al,[67] Ni[68]) and nonmetals (C,[69] N[70]) in liquid calcium and the morphology of alloy particles between them.

Table S10 (see the electronic supplementary data file) shows that the insoluble metals have spongy particles after reduction (Ti,[71] Zr,[72] Hf,[33,73] Nb, and Ta[39]). The same is true for binary alloys, such as V-30 at pct Ti[74] and Cr_2Ti[30] (the spongy morphology of calciothermic Ti and Cr_2Ti particles is demonstrated in Figure S11 (see the electronic supplementary data file) in Supplementary Materials). If one of the components is highly soluble in calcium, then the morphology of the synthesized powders is determined by the chemical composition of the alloy (in at pct). For example, Ti_3Al (~ 75 at pct Ti)[75] and Nb_3Al (~ 75 at pct Nb)[31] powders, the basis of which is a calcium-insoluble metal, have a spongy particle shape (see electronic supplementary Figure S12). At the same time, the compound $NbAl_3$ (~75 at pct Al) based on Al, which is highly soluble in liquid calcium, has a globular particle shape.[76] Those powder alloys that consist only of calcium-soluble elements, for example, NiAl or Ni_3Al,[77] have globular particle shape (see electronic supplementary Figure S13). An interesting case is the calcium-hydride synthesis of refractory carbides or carbonitrides. In such case, the special synthesis mechanism causes the formation of cubic nanoparticles of Zr, Hf, Nb, or Ta carbides and Hf(C,N) carbonitride[33,78] (see electronic supplementary Figure S14). Thus, it should be noted that the typical morphology of the calciothermic (calcium-hydride) powders of metals and alloys insoluble in liquid calcium is spongy.

G. *Morphological Features of Diffusion Formation of Cr_2Ta*

There is every reason to expect that the morphology of Cr_2Ta particles will be spongy, and the excess of the reducing agent (liquid phase Ca) should not have any effect on this morphology, since neither Cr nor Ta is soluble in liquid Ca. Due to the fact that the process of the formation of the Cr_2Ta phase is controlled by solid-state diffusion of Cr into Ta (Figure 5), the Cr_2Ta intermetallic compound will inherit the morphology of reduced Ta particles.

Figure 9a, b demonstrates the morphology of the parent oxides Cr_2O_3 and Ta_2O_5. It can be seen that the Cr_2O_3 particles have a smooth, near-globular shape (Figures 9a). Ta_2O_5 oxide, on the contrary, has a more complex morphology. There are (Figures 9b) both monolithic (smooth, rough) and porous (near-globular) particles. The particle size of the oxide powders is very small about ~2.54 μm for Cr_2O_3 and ~ 2.80 μm for Ta_2O_5 (geometric mean). After the calcium-hydride reduction of Cr_2O_3 oxide, Cr particles with a size of about 5–10 μm have been observed (Figures 9c, d, g, i). However, it is worth noting that these data cannot be used to claim that large Cr powder is formed by the reduction of Cr_2O_3, since most of its particles were consumed for the formation of the Cr_2Ta phase, the size of which cannot be taken into account. Figure 9c, d, g, i shows unreacted Cr particles. The reduction of Ta_2O_5 results in the formation of similar in size but spongy Ta particles (Figures 9f,g).

Figure 9c through k illustrates the structure of Cr_2Ta powder particles obtained in a temperature range of 970–1200 °C and with various excess of reducing agent under an isothermal holding of 240 minutes.

As expected, the excess of the reducing agent has no effect on the particle morphology of the synthesized Cr_2Ta powders (Figures 9a through c). The results have shown that the intermetallic compound has a spongy morphology with a size of less than 20 μm. Quite large particles belonging to Cr have also been observed, which are in good agreement with the phase analysis data (Figures 2b).

The powders synthesized at temperatures ranging from 970 to 1000 °C (Figures 9f, g) displayed a minimal presence of Cr_2Ta phases, with their metallic phases primarily composed of Ta and Cr (see electronic supplementary Table S3). It has been observed that the reduced Ta particles displayed a complex, spongy morphology, while the reduced Cr particles are characterized by large, smooth particles (Figures 9h, k). This spongy morphology of Ta particles can be seen in Figure 9 (depicting reduction at 970 and 1000 °C). As the reduction temperature is increased up to 1200 °C, it is observed that the spongy morphology of the particles is retained, but the presence of the Cr_2Ta intermetallic compound is now evident (Figures 9h through k).

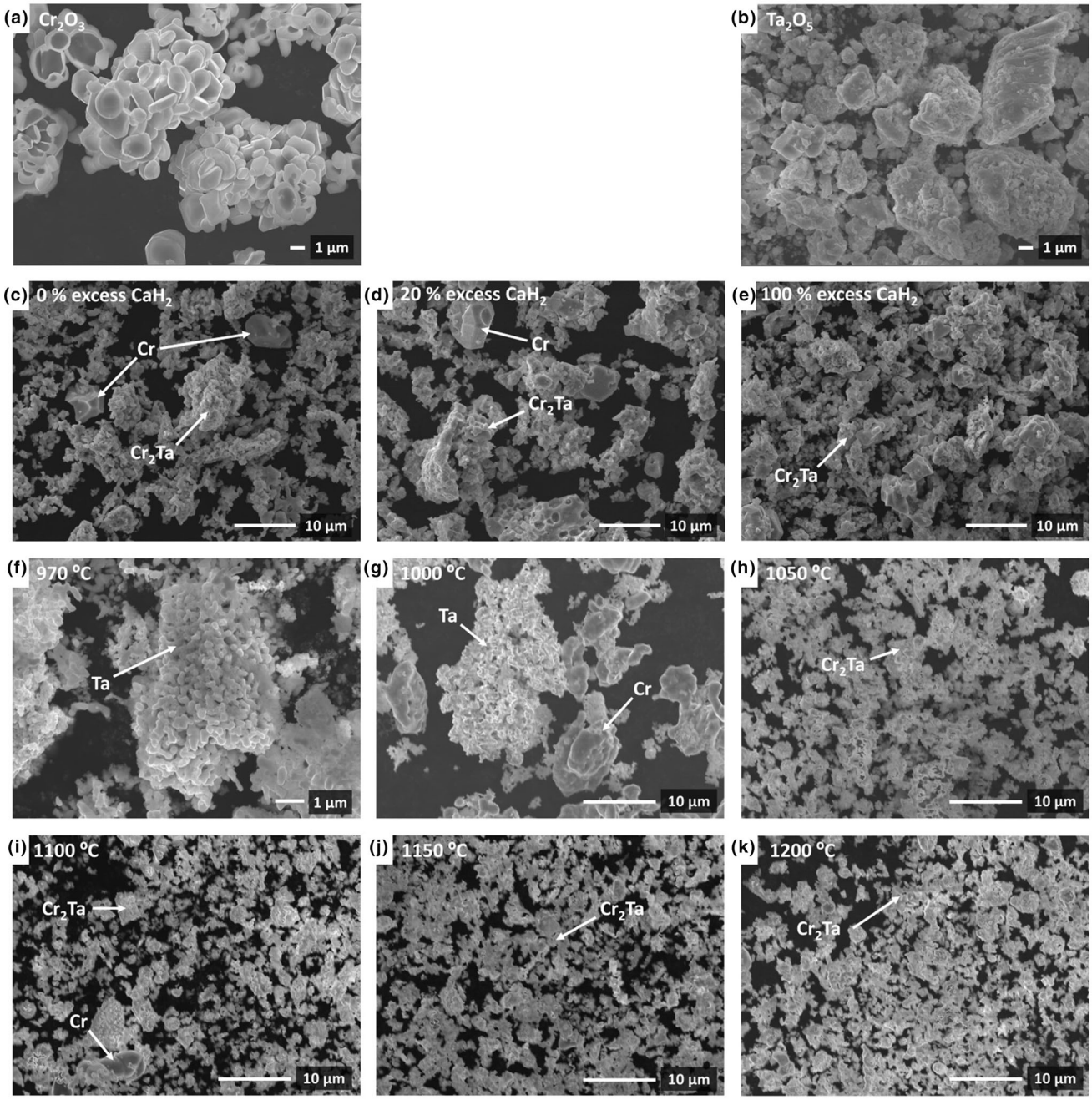

Fig. 9—Morphology of the oxides (*a*, *b*) and Cr_2Ta powders synthesized: (*c* through *e*) at 1200 °C for 360 min and a CaH_2 excess of 0, 20, and 100 wt pct; (f through k) in the temperature range of 970–1200 °C for 240 min and CaH_2 excess of 20 wt pct.

However, with increasing temperature, the coarsening process due to sintering begins to take effect (see electronic supplementary Table S15). The grains lose their individual characteristics, porosity within the agglomerate decreases, and the particles begin to approach one another. No significant structural changes in the particles of the synthesized Cr_2Ta powders beyond those expected through the simple theory of sintering were observed. It has been previously reported in the literature[72,74] that spongy calciothermic powders exhibit active sintering, resulting in a decrease of porosity and approach of particles within the agglomerate. This is consistent with the observations made in the current study.

H. *Oxides and Carbides in Cr_2Ta Powders*

The presence of impurity oxide and carbide phases can greatly impact the properties of materials. Figures 10a illustrates the effect of temperature and reduction time on the concentration of oxide phases in Cr_2Ta powders synthesized using calcium hydride.

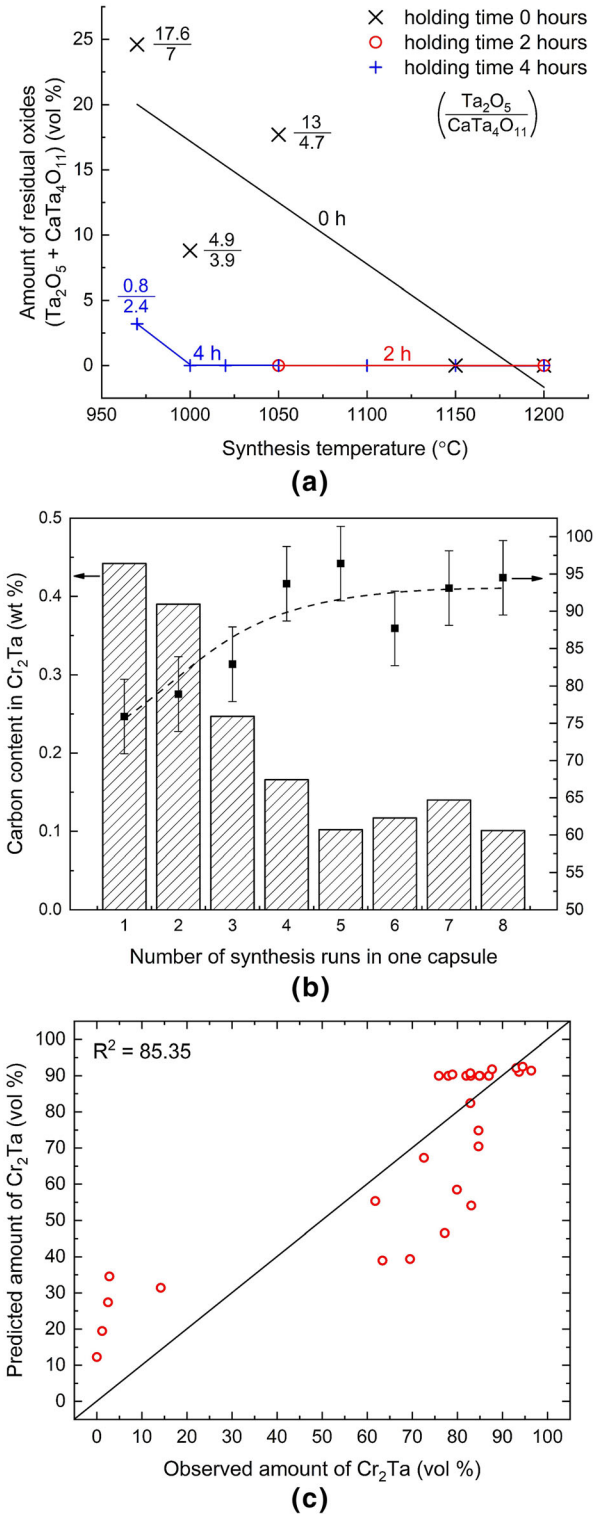

Fig. 10—(*a*) Influence of temperature–time conditions of the calcium-hydride reduction on the content of oxide phases in Cr_2Ta powders. In parentheses, the numerator shows the Ta_2O_5 content (vol pct), the denominator—$CaTa_4O_{11}$; (*b*) The effect of the number of runs in the same capsule on the carbon content in the synthesized powders; (c) Predictive power of the regression model Eq. [3].

Oxide phases are only observed at short reduction times and temperatures (as shown in Figures 10a). The presence of the complex oxide phase $CaTa_4O_{11}$ confirms the multi-stage nature of Ta_2O_5 oxide, as previously reported in the literature.[59] Based on X-ray phase analysis (Figures 2d), it can be seen that at the maximum temperature and reduction time, the Cr_2Ta phase is not present in 100 pct concentration. Additionally, theoretical calculations performed using formula [2] indicate that a temperature of ~ 1190 °C might be sufficient to fully form the Cr_2Ta compound under the conditions of the calcium-hydride synthesis. However, the highest concentration of Cr_2Ta achieved was 85 pct by volume. The remaining 15 pct of the powder was composed of carbide phases Ta_2C and TaC (up to ~ 10 pct by volume) and residual unreacted metals Cr and Ta (up to ~ 5 pct by volume). It has been observed that the incorporation of Ta into refractory carbides precludes its interaction with chromium particles, thereby suppressing the formation of the Cr_2Ta phase.

In the calcium-hydride technology, spacers made of ordinary carbon steel containing up to 0.26 wt pct. C are often employed to separate the charge from the container walls, which are made of chromium-nickel heat-resistant steel (Figure 1). This prevents contamination of the alloy powder with nickel, as nickel is highly soluble in liquid calcium (see electronic supplementary Table S10). Conversely, iron is virtually insoluble in liquid calcium, making steel a suitable and uncomplicated material for defining the reaction volume.

It is possible that carbon from the steel reacts with the reduced Ta particles that come into contact with the capsule walls. To test this hypothesis, a series of experiments was conducted at the maximum synthesis temperature (1200 °C) and holding time (360 minutes) in the same reaction capsule (experiments Nos. 22-29 in Table I) for a total of 8 consecutive trials. The results are presented in Figure 10.

Figure 10b demonstrates that following the initial synthesis run, the powder was contaminated with carbon to an extent of ~ 0.45 wt pct, with a Cr_2Ta phase present at a volume fraction of 75 pct. The subsequent synthesis runs showed a decrease in carbon concentration by ~ 0.1 wt pct/run and an increase in the proportion of the Cr_2Ta phase by ~ 6 vol pct/run. This trend was observed for the first five synthesis runs, implying a negative correlation between carbon content and target product concentration. Beginning with the fifth experiment, the carbon and Cr_2Ta phase concentrations stabilized at ~ 0.11 wtpct and ~ 95 vol pct, respectively. The results indicate that utilizing ordinary carbon steel as a tooling material results in the contamination of the Cr_2Ta powder with carbon. However, the use of low-carbon steel (tin) enables the synthesis of a material with a desired phase content of 95 ± 5 vol pct.

When implementing the calcium-hydride regimes to produce Cr_2Ta using standard and low-cost steel equipment, it is crucial to consider the competition between carbon and chromium for tantalum and to prevent

carbon contamination. To achieve this, crucibles made of low-cost sheet metal or refractory metals such as Nb, Ta, or Mo should be utilized.[39,74–76] The results showed that Cr_2Ta powders synthesized at a temperature of 1200 °C for 360 °C contain oxygen in an amount of 0.20–0.28 wt pct and nitrogen in an amount of 0.05 – 0.08 wt pct (see electronic supplementary Table S16).

I. *Regression Model of the Cr_2Ta Synthesis*

Its application in the fine tuning of intermetallics synthesis through regression models has the potential facilitate the understanding of complex relationships between variables and to pave the way for producing materials of exceptional quality with optimal properties. Harnessing the power of regression models, this technique facilitates precise control of the synthesis process, thereby enabling unprecedented advancements in material science. In the case of the Cr_2Ta synthesis, regression modeling was used to provide insights into the influence of the temperature (T, °C), holding time (τ, min), reducing agent excess (Ex, pct), and the number of runs (R) in one capsule to help describe the synthesis and enable optimization of reaction conditions. The following regression model of the synthesis of Cr_2Ta (Eq. [3]) was developed using the Minitab 21 software:

$$Q_{Cr_2Ta} = -220.0 + 0.2391 \cdot T + 0.063 \cdot \tau + 0.36 \cdot R. \quad [3]$$

The adequacy of model (3) is shown in Figures 10c.

Using Eq. [3], it is possible to calculate the reduction temperature (T) at which it will be possible to obtain a Cr_2Ta powder with 100 pct of the desired phase. By taking the exposure time (τ) of 360 minutes and the number of modes in the same capsule (R) equal to 8 as boundary conditions, the synthesis temperature of 1231 °C was calculated as required to obtain 100 pct of Cr_2Ta, which agrees well with the present experimental data (Figures 2c, 6a and 10b). In addition, the value of 1231 °C is quite close to the temperature of 1190 °C, at which 100 pct of the Cr_2Ta compound should also be formed, according to the Arrhenius Eq. [2]. Probably, all this indicates an adequately defined mechanism for the formation of the Cr_2Ta intermetallic compound (solid-state diffusion) and the admissibility of using these numerical methods for calculating the amount of the Cr_2Ta phase.

With accordance to the effect of each factor on the Cr_2Ta content, the synthesis parameters can be arranged in a following sequence: reduction temperature, holding time, runs in the same capsule, a reducing agent excess (see electronic supplementary Figure S17). The strongest effect on the Cr_2Ta content possesses reduction temperature. The excess of reducing agent is statistically considered an insignificant factor.

To facilitate the optimization of the microkinetic parameters of the synthesis process, we visualized the regression model as three contour plots (Figures 11a through c).

III. CONCLUSIONS

Regression analysis and experimental studies have identified the main factors of the calcium-hydride synthesis affecting the quality of Cr_2Ta powders, which, according to their degree of influence, can be arranged as follows: Synthesis temperature → synthesis duration → number of runs in one capsule →excess reducing agent. The conclusions are described as follows:

1. During the reduction of Cr_2O_3 and Ta_2O_5 oxides, Cr and Ta interact diffusely with each other in the solid phase, displaying an activation energy of 291 ± 69 kJ/mol. The kinetics of the solid-phase reaction ($2Cr + Ta \rightarrow Cr_2Ta$) was found to be governed by the three-dimensional mass transfer of chromium into tantalum particles.
2. Significant acceleration in the rate of Cr_2Ta formation was observed when the reduction temperature was elevated above 1000 °C. The differential scanning calorimetry (DSC) experiments suggest that this phenomenon may be attributed to the action of a chemical heat source, which was generated during the highly exothermic reaction $Cr_2O_{3solid} + 3Ca_{liq-}$

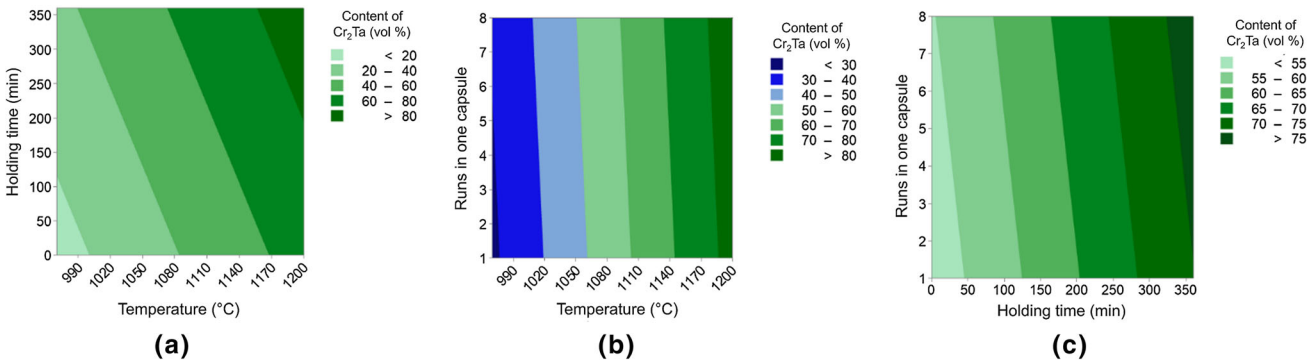

Fig. 11—Contour plots corresponding to the yield of Cr_2Ta depending on the combination of (*a*) holding time and temperature (hold value = 2 runs in one capsule); (*b*) number of runs in one capsule and temperature (hold value = 250 min); (*c*) number of runs in one capsule and holding time (hold value = temperature 1136 °C).

$_{uid} \rightarrow 2Cr_{solid} + 3CaO_{solid}$, thus, increasing the reaction rate.

3. Moreover, it was established that the excess amount of reducing agent (up to 100 pct) did not have a significant effect on the morphology and phase composition of the Cr_2Ta powders. The shape of Cr_2Ta particles was found to inherit the morphology of reduced Ta.
4. It was discovered that the particles of reduced Ta in contact with the steel tooling (capsules) walls interact with the carbon present in the steel to form Ta_2C and TaC carbides. To mitigate this issue, it was concluded that the use of tooling that does not contain carbon would ensure complete chromium-tantalum reaction and decrease the residual carbon concentration in the powders from 0.50 to < 0.10 wt pct.
5. In order to achieve a powder with a phase content of 95 ± 5 vol pct, the following technological parameters must be employed for calcium-hydride reduction: a temperature of 1200 °C, a minimum holding time of 360 minutes, an excess of the reducing agent of 20 wt pct, and the use of carbon-free iron or pure refractory metals (such as Nb, Mo, etc.) as a reaction capsule.

ACKNOWLEDGMENTS

This work was supported by the Russian Science Foundation (project no. 22-23-20113) and the Tula Oblast Committee for Science and Innovations (grant no. 3, April 19, 2022)

COMPETING INTEREST

The authors declare that they have no known competing financial interests or personal relationships that could have appeared to influence the work reported in this paper.

SUPPLEMENTARY INFORMATION

The online version contains supplementary material available at https://doi.org/10.1007/s11663-024-03018-0.

REFERENCES

1. H. Bei, G.M. Pharr, and E.P. George: *J. Mater. Sci.*, 2004, vol. 39, pp. 3975–984.
2. D.L. Anton, D.M. Shah, D.N. Duhl, and A.F. Giamei: *JOM*, 1989, vol. 41, pp. 12–7.
3. D.J. Duquette and N.S. Stoloff: *Key Eng. Mater.*, 1992, vol. 77–78, pp. 289–304.
4. C.T. Liu: *Mater. Chem. Phys.*, 1995, vol. 42, pp. 77–86.
5. G.H. Meier and F.S. Pettit: *Mater. Sci. Technol.*, 1992, vol. 8, pp. 331–38.
6. H. Zheng, S. Lu, Z. Jianye, and L. Guangming: *Int. J. Refract. Metals Hard Mater.*, 2009, vol. 27, pp. 659–63.
7. J.H. Westbrook and R.L. Fleischer: *Intermetallic Compounds: Structural Applications of Intermetallic Compounds*, vol. 3, Wiley, New York, 2000, p. 346.
8. J.D. Livingston: *Phys. Status Solidi A*, 1992, vol. 131, pp. 415–23.
9. H. Zheng, S. Cheng, X. Shu, and G. Li: *Int. J. Refract. Metals Hard Mater.*, 2017, vol. 66, pp. 57–62.
10. C. Li, J.L. Hoe, and P. Wu: *J. Phys. Chem. Solids*, 2003, vol. 64, pp. 201–12.
11. A. Von Keitz and G. Sauthoff: *Intermetallics (Barking)*, 2002, vol. 10, pp. 497–510.
12. C.T. Liu, J. Stringer, J.N. Mundy, L.L. Horton, and P. Angelini: *Intermetallics (Bark.)*, 1997, vol. 5, pp. 579–96.
13. J.H. Perepezko, C.A. Nuñes, S.-H. Yi, and D.J. Thoma: *MRS Proc.*, 1996, vol. 460, pp. 3–14.
14. M. Venkatraman and J.P. Neumann: *J. Phase Equilib.*, 1987, vol. 8, pp. 112–16.
15. S. Hong, C.L. Fu, and M.H. Yoo: *Intermetallics (Bark.)*, 1999, vol. 7, pp. 1169–172.
16. A.S. Dorcheh and M.C. Galetz: *JOM*, 2016, vol. 68, pp. 2793–802.
17. M.P. Brady, P.F. Tortorelli, and L.R. Walker: *Mater. High Temp.*, 2000, vol. 17, pp. 235–41.
18. M.P. Brady, J.H. Zhu, C.T. Liu, P.F. Tortorelli, and L.R. Walker: *Intermetallics (Bark.)*, 2000, vol. 8, pp. 1111–118.
19. A. Bhowmik and H.J. Stone: *Metall. Mater. Trans. A*, 2012, vol. 43, pp. 3283–292.
20. N. Dupin and I. Ansara: *J. Phase Equilib.*, 1993, vol. 14, pp. 451–56.
21. A. Bhowmik, C.N. Jones, I.M. Edmonds, and H.J. Stone: *J. Alloys Compd.*, 2012, vol. 530, pp. 169–77.
22. C.T. Liu, J.H. Zhu, M.P. Brady, C.G. McKamey, and L.M. Pike: *Intermetallics (Bark.)*, 2000, vol. 8, pp. 1119–129.
23. H.-J. Lunk: *ChemTexts*, 2015, vol. 1, p. 6.
24. J.W. Arblaster: *J. Phase Equilib. Diffus.*, 2018, vol. 39, pp. 255–72.
25. V.K. Portnoi, A.V. Leonov, S.E. Filippova, A.I. Logacheva, A.G. Beresnev, and I.M. Razumovskii: *Inorg. Mater.*, 2016, vol. 52, pp. 895–901.
26. G.A. Meerson and O.P. Kolchin: *Soviet J. Atomic Energy*, 1957, vol. 2, pp. 305–12.
27. O. Kubaschewski and W.A. Dench: *J. Inst. Met.*, 1954, vol. 82, pp. 87–91.
28. O. Kubaschewski and W.A. Dench: *J. Inst. Metals*, 1956, vol. 84, pp. 440–44.
29. S. Liu, R.O. Suzuki, and K. Ono: *J. Alloys Compd.*, 1998, vol. 266, pp. 247–54.
30. O. Bayat, A.R. Khavandi, and R. Ghasemzadeh: *J. Alloys Compd.*, 2012, vol. 520, pp. 164–69.
31. S.N. Yudin, A.V. Kasimtsev, A.V. Korotitskiy, T.A. Sviridova, G.V. Markova, S.S. Volodko, A.A. Nepapushev, and D.O. Moskovskikh: *Mater. Sci. Eng. A*, 2020, vol. 790, 139715.
32. S. Yudin, I. Alimov, S. Volodko, A. Gurianov, G. Markova, A. Kasimtsev, T. Sviridova, D. Permyakova, E. Evstratov, V. Cheverikin, and D. Moskovskikh: *J. Funct. Biomater.*, 2023, vol. 14, p. 271.
33. S.N. Yudin, A.V. Kasimtsev, S.S. Volodko, I.A. Alimov, G.V. Markova, T.A. Sviridova, N.Y. Tabachkova, V.S. Buinevich, A.A. Nepapushev, and D.O. Moskovskikh: *Materialia (Oxf)*, 2022, vol. 22, 101415.
34. A.V. Kasimtsev, S.N. Yudin, and Yu.V. Levinsky: *Non-ferrous Metals*, 2020, vol. 49, pp. 31–50.
35. E.V. Shelekhov and T.A. Sviridova: *Met. Sci. Heat Treat.*, 2000, vol. 42, pp. 309–13.
36. H.M. Rietveld: *J. Appl. Crystallogr.*, 1969, vol. 2, pp. 65–71.
37. W.C. Johnson, M.F. Stubbs, A.E. Sidwell, and A. Pechukas: *J. Am. Chem. Soc.*, 1939, vol. 61, pp. 318–29.
38. D.T. Peterson and V.G. Fattore: *J. Phys. Chem.*, 1961, vol. 65, pp. 2062–64.
39. M. Baba, Y. Ono, and R.O. Suzuki: *J. Phys. Chem. Solids*, 2005, vol. 66, pp. 466–70.
40. R.O. Suzuki and Y. Matsuoka: in *Proceedings of the JGSEE and Kyoto University Joint International Conference on Sustainable Energy and Environment (SEE). Hua-Hin, Thailand, December 1-3, 2004*, Joint Graduate School of Energy and Environment (JGSEE), 2004, pp. 167–170.
41. D. Naoi and M. Kajihara: *Mater. Sci. Eng. A*, 2007, vol. 459, pp. 375–82.

42. S. Horiuchi and R. Blanchard: *Solid State Electron*., 1975, vol. 18, pp. 529–32.
43. J.C. Liu, J.W. Mayer, and J.C. Barbour: *J. Appl. Phys*., 1988, vol. 64, pp. 656–62.
44. J. Šesták and G. Berggren: *Thermochim. Acta*, 1971, vol. 3, pp. 1–2.
45. S. Gupta, R. Kumar, S. Majumdar, J. Sonber, S.K. Satpati, and M.L. Sahu: *J. Alloys Compd*., 2019, vol. 791, pp. 109–20.
46. G. Qi, M. Hino, and A. Yazawa: *Mater.Trans. JIM*, 1990, vol. 31, pp. 463–70.
47. B. Freudenberg and A. Mocellin: *J. Am. Ceram. Soc*., 1988, vol. 71, pp. 22–8.
48. G.E. Vignoul, J.K. Tien, and J.M. Sanchez: *Mater. Sci. Eng. A*, 1993, vol. 170, pp. 177–83.
49. W. Baumann, A. Leineweber, and E.J. Mittemeijer: *Intermetallics (Bark.)*, 2011, vol. 19, pp. 526–35.
50. V.A. Baheti, S. Roy, R. Ravi, and A. Paul: *Intermetallics (Bark.)*, 2013, vol. 33, pp. 87–91.
51. M. Denkinger and H. Mehrer: *Philos. Mag. A*, 2000, vol. 80, pp. 1245–263.
52. M. Wein, L. Levin, and S. Nadiv: *Philos. Mag. A*, 1978, vol. 38, pp. 81–96.
53. A.V. Kasimtsev and V.V. Zhigunov: *Russ. J. Non-Ferrous Metals*, 2010, vol. 51, pp. 150–57.
54. A.V. Kasimtsev, S.S. Volodko, S.N. Yudin, T.A. Sviridova, and V.V. Cheverikin: *Inorg. Mater*., 2019, vol. 55, pp. 449–57.
55. A.V. Kasimtsev and V.V. Zhigunov: *Russ. J. Non-Ferrous Metals*, 2008, vol. 49, pp. 471–77.
56. J.A. Dean and Norbert Adolph Lange: *Lange's Handbook of Chemistry: Fifteenth Edition*, 15th edn., McGraw-Hill Professional, New York, 1999, pp. 1538.
57. J.N. Dzneladze, R.P. Shchegoleva, L.G. Golubeva, E.M. Rabinovich, and B.A. Borok B.A.: *Poroshkovaya Metallurgiya Stalei i Splavov [Powder Metallurgy of Steels and Alloys] (in Russian)*, Metallurgiya, Moscow, 1978, pp. 264.
58. R.W. Curtis and P. Chiotti: *J. Phys. Chem*., 1963, vol. 67, pp. 1061–65.
59. K.T. Jacob and A. Rajput: *J. Alloys Compd*., 2015, vol. 620, pp. 256–62.
60. A.S. Rogachev, A.N. Gryadunov, N.A. Kochetov, A.S. Schukin, F. Baras, and O. Politano: *Int. J. Self Propag. High Temp. Synth*., 2019, vol. 28, pp. 196–98.
61. A.S. Rogachev, S.G. Vadchenko, N.A. Kochetov, DYu. Kovalev, I.D. Kovalev, A.S. Shchukin, A.N. Gryadunov, F. Baras, and O. Politano: *J. Eur. Ceram. Soc*., 2020, vol. 40, pp. 2527–532.
62. Y. Li, Q. Liu, and W. Shen: *Dalton Trans*., 2011, vol. 40, p. 5811.
63. I. Obinata, Y. Takeuchi, and S. Saikawa: *Phys Chem. Metall*., 1960, vol. 12, pp. 470–70.
64. K.-H. Wu, Y. Wang, K.-C. Chou, and G.-H. Zhang: *Int. J. Refract. Metals Hard Mater*., 2021, vol. 98, 105567.
65. B. Predel: *Ca-Cd–Co–Zr*, Springer, Berli, 2005, pp. 1-.
66. M. Venkatraman and J.P. Neumann: *Bull. Alloy Phase Diagr*., 1985, vol. 6, pp. 335–35.
67. V.P. Itkin, C.B. Alcock, P.J. van Ekeren, and H.A.J. Oonk: *Bull. Alloy Phase Diagr*., 1988, vol. 9, pp. 652–57.
68. M. Notin, D. Belbacha, M. Rahmane, J. Hertz, G. Saindrenan, and J.L. Jorda: *J. Less Common Metals*, 1990, vol. 162, pp. 221–29.
69. P. Villars, M. Berndt, K. Brandenburg, K. Cenzual, J. Daams, F. Hulliger, T. Massalski, H. Okamoto, K. Osaki, A. Prince, H. Putz, and S. Iwata: *J. Alloys Compd*., 2004, vol. 367, pp. 293–97.
70. V.P. Itkin and C.B. Alcock: *J. Phase Equilib*., 1990, vol. 11, pp. 497–503.
71. K. Ono: *Mater. Trans*., 2004, vol. 45, pp. 1660–664.
72. A.M. Abdelkader and E. El-Kashif: *ISIJ Int*., 2007, vol. 47, pp. 25–31.
73. A.M. Abdelkader and A. Daher: *J. Alloys Compd*., 2009, vol. 469, pp. 571–75.
74. R.O. Suzuki, K. Tatemoto, and H. Kitagawa: *J. Alloys Compd*., 2004, vol. 385, pp. 173–80.
75. R.O. Suzuki, M. Ikezawa, T.H. Okabe, T. Oishi, and K. Ono: *Mater. Trans. JIM*, 1990, vol. 31, pp. 61–8.
76. T.H. Okabe, K. Fujiwara, T. Oishi, and K. Ono: *Metall. Trans. B*, 1992, vol. 23, pp. 415–21.
77. A.V. Kasimtsev and T.A. Sviridova: *Russ. Metall. (Metally)*, 2012, vol. 2012, pp. 435–44.
78. S. Yudin, S. Volodko, D. Moskovskikh, I. Alimov, A. Guryanov, S. Zhevnenko, H. Guo, A. Korotitsky, K. Sidnov, S. Roslyakov, and C. Zhang: *J. Eur. Ceram. Soc*., 2023, vol. 43, pp. 5108–116.